Twenty-Sixth Symposium (International) on Combustion/The Combustion Institute, 1996/pp. 1275–1281

INFLUENCE OF GRAVITY ON THE PROPAGATION OF INITIALLY SPHERICAL FLAMES

J. DAOU AND B. ROGG
Institut für Thermo- und Fluiddynamik
Ruhr-Universität, D-44780 Bochum, Germany

We study the evolution of an initially spherical kernel of burned gas in a fresh reactive mixture in the presence of a gravity field. The study is carried out numerically in the framework of an axisymmetric geometry, the chemistry being modeled by an irreversible overall one-step reaction. Attention is focused on the influence of two nondimensional parameters, namely the reciprocal of the Froude number, Fr^{-1}, and the Lewis number *Le*. Dependencing on these parameters, many different flame shapes are observed. The influence of *Le* is found to be consistent with the present knowledge on stretched flames: For $Le < 1$, an important reduction in the reaction rate is observed at the back of the hot deformed kernel, which can lead to extinction there. For $Le > 1$, the same occurs at the front surface but typically the flame persists at the back. For $Le = 1$, the combustion characteristics, such as the combustion temperature, are found to be practically independent of Fr^{-1}, up to very high values of this parameter.

A simple model based on a potential flow assumption in the fresh gas is developed and used to evaluate *locally* the numerically predicted flow field and hence the local stretch over the flame surface. For intermediate values of Fr^{-1}, as they are typical in the case of weak kernel deformation, this model is shown to be valid over the entire flame surface. Finally, the relevance of our study to experimental results, which are mainly concerned with flammability limits, is discussed.

Introduction

Over the past decades in combustion research, there has been increasing interest in the effects of gravity on various aspects of combustion such as flammability limits, [1–7], flame stability, [8,9], and droplet combustion. Nevertheless, gravity has remained a quantity whose influence on combustion is still difficult to quantify. In theoretical and, to a lesser extent, in numerical investigations, this is so because the inclusion of gravity in the governing equations renders their solution much more difficult. In experimental research it is the opposite: here the presence of gravity is natural but major efforts are undertaken to conduct experiments in reduced-gravity, down to microgravity, conditions. Because of these difficulties in theory, numerics and, experiments, the effects of gravity on combustion are still not sufficiently understood.

The purpose of the present paper is to contribute to a better basic understanding of the effects of gravity, in particular with respect to their influence on the flow and flame dynamics and on their interactions with differential diffusion. To this end, we study the propagation of an initially spherical premixed flame surrounding a kernel of hot combustion products under the influence of gravity. Because of the physicochemical complexity, which arises mainly from the coupling between the flow and the flame, and in order to facilitate the physical understanding of the phenomena observed, the model is kept as simple as possible. Thus, geometrical simplifications are achieved by assuming axial symmetry, a simplified version of the thermophysical properties is adopted, and the chemistry is modeled by an overall irreversible one-step reaction.

The paper is organized as follows. First, we present the physical model. Here the governing equations are given in nondimensional form, and the nondimensional parameters of the problem are identified. Of these, in the present study, the nondimensional activation energy, that is, the Zeldovich number, and a gas-expansion parameter or heat-release parameter, the Prandtl number, and the nondimensional initial kernel radius are kept fixed, whereas the Froude number, which herein is characterized by its reciprocal Fr^{-1}, and the Lewis number, *Le*, are taken as variable parameters. The unsteady governing equations in cylindrical coordinates are solved numerically for a wide range of Froude and Lewis numbers. In the presentation of results, we first consider typical cases corresponding to $Le = 1$ but to different values of Fr^{-1}, thereby revealing the influence of the strength of gravity on the aerodynamic characteristics of the flame. Then the influence of the Lewis number on flame propagation is studied. Here, to complement and help interpret the numerically obtained results, a simple potential-flow model is developed, which provides analytical expressions for flame stretch and flame temperature.

Finally, the relevance of the numerical results is discussed in the context of flammability limits.

Model

We consider the evolution of an initially spherical, laminar premixed flame surrounding a pocket of burned gas in a fresh reactive mixture in the presence of gravity. To focus attention on the main physical aspects and to achieve simplifications in the governing equations, the following assumptions are adopted. Low Mach number flow, which is axisymmetric with the symmetry axis being co-linear with gravity, is considered. Combustion is modeled by a single irreversible reaction between two reactants. (We note that this assumption on chemistry is not essential in that the overall model is readily extended to include more detailed chemistry models, such as systematically reduced kinetic mechanisms or detailed kinetic mechanisms of elementary reactions.) Specifically, mixtures are considered that are sufficiently off stoichiometric (either lean or rich) for concentration variations of the nondeficient reactant to be neglected, so that (1) variations in the mixture molecular weight are negligibly small and (2) only the species conservation equation of the deficient species needs to be considered. The reaction rate is assumed to be of Arrhenius form. Thus, it is taken as proportional to the density, to the mass fraction of the deficient species, and to $B\ \exp(-E/R^0T)$, where B denotes the constant preexponential factor, E is the activation energy, R^0 the universal gas constant, and T the temperature. Thermal conductivity λ, heat capacity c_p, dynamic viscosity μ, and the product of the density with a suitably defined diffusion coefficient of the deficient reactant are taken as constant. Effects of thermal diffusion, viscous dissipation and radiative heat losses are justifiably neglected. As reference quantities for nondimensionalization we select the laminar flame thickness l_F^0, the laminar flame velocity S_L^0, and the density of the fresh mixture.

With the preceding assumptions, and using the given reference quantities, the conservation equations in nondimensional form can be written as

$$\frac{\partial \rho}{\partial t} + \nabla\cdot(\rho \boldsymbol{v}) = 0 \tag{1}$$

$$\rho\frac{\partial \boldsymbol{v}}{\partial t} + \rho\boldsymbol{v}\cdot\nabla\boldsymbol{v} = -\nabla p + Pr\Delta\boldsymbol{v} + Fr^{-1}(1-\rho)\boldsymbol{e}_x \tag{2}$$

$$\rho\frac{\partial \theta}{\partial t} + \rho\boldsymbol{v}\cdot\nabla\theta = \Delta\theta + \Omega \tag{3}$$

$$\rho\frac{\partial Y}{\partial t} + \rho\boldsymbol{v}\cdot\nabla Y = Le^{-1}\,\Delta Y - \Omega \tag{4}$$

where ρ, t, ∇, Δ, v, and p are nondimensional but otherwise have their usual meaning; $Pr = \mu c_p/\lambda$ denotes the Prandtl number, and $Fr \equiv S_L^{0\,2}/(gl_F^0)$, where g is the modulus of the gravity vector $\boldsymbol{g}$, is the Froude number; $\boldsymbol{e}_x\ (= -\boldsymbol{g}/g)$ denotes the unit vector in the x direction and $\theta = (T - T_u)/(T_{\rm ad} - T_u)$ is a nondimensional temperature; here T_u is the temperature in the fresh reactants and $T_{\rm ad}$ is the corresponding adiabatic flame temperature; ρ and θ are linked by the ideal-gas equation of state,

$$\rho = \left(1 + \frac{\gamma}{1-\gamma}\,\theta\right)^{-1} \tag{5}$$

where γ denotes a gas-expansion or heat-release parameter, $\gamma = (T_{\rm ad} - T_u)/T_{\rm ad}$; Y denotes the mass fraction of the deficient reactant normalized by its value in the fresh mixture. The nondimensional reaction term Ω is given by

$$\Omega = \rho Y\frac{\beta^2}{2Le(1-\gamma)}\exp\left[\frac{-\beta(1-\theta)}{1+\gamma(\theta-1)}\right] \tag{6}$$

where β is the Zeldovich number and Le the Lewis number. In Eq. (6), use has been made of the asymptotic result

$$S_L^0 = \sqrt{2Le(1-\gamma)/\beta^2\ a_u B\ \exp(-E/R^0T_{\rm ad})}$$

here a_u denotes the thermal diffusivity of the fresh, reactive mixture.

Eqs. (1) through (4) are to be supplemented by suitable initial and boundary conditions. To this end, herein an initially spherical flame ball of nondimensional initial radius R_0, consisting of hot combustion products at adiabatic flame temperature, is placed into an initially quiescent reactive mixture. Inside the flame ball, the initial values $\theta = 1$, $Y = 0$, and $\boldsymbol{u} = \boldsymbol{0}$ are selected; outside it, the values are $\theta = 0$, $Y = 1$, $\boldsymbol{u} = \boldsymbol{0}$. The boundary conditions are taken to correspond to a stagnant fresh gas at infinity, with a prescribed temperature and composition, that is, $\theta = 0$, $Y = 1$, and $\boldsymbol{u} = \boldsymbol{0}$. In the present study, all computations were performed for $R_0 = 10$, $Pr = 1$, $\gamma = 0.85$, and $\beta = 5$.

Numerical Considerations

Space limitations in the present volume do not permit us to include details of the numerical solution approach. Therefore, only a brief outline of numerical considerations can be given here. Eqs. (1) through (4), in cylindrical coordinates, are first discretized using a finite volume method and then solved with a multigrid method [10]. The extent of the computational domain in both the axial and radial direction is finite but large compared to the initial flame-ball radius. After each time step, the solution of the governing equations is remapped to the domain such that the flame remains located

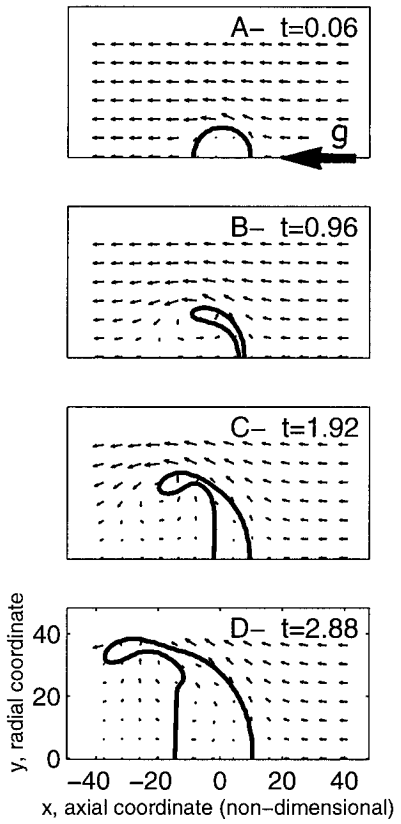

FIG. 1. Flame deformation and expansion for $Fr^{-1} = 100$, $Le = 1$ and $R_0 = 10$. The flame is represented by the temperature contour $\theta = 0.95$. Arrows show the velocity field relative to a frame moving with the average velocity of the hot kernel. The pictures pertain, respectively, to nondimensional time $t = 0.06$, 0.96, 1.92, and 2.88.

approximately at the origin of the coordinate system. The grid is a nonuniform tensor-product grid, typically with 400 × 200 grid points.

Results and Discussion

Because of space limitations, only a few typical results of the many more obtained can be presented here. Presentation of results is structured as follows. First, the influence of the strength of gravity is studied for flames with a Lewis number of unity, thereby eliminating the effects of differential diffusion on the flame characteristics. Second, the effects of differential diffusion are investigated. To this end, first a simple potential-flow model is developed that aids in the qualitative understanding of the numerical results. Then, the effects of differential diffusion are discussed for weak flame deformation as it occurs for small-to-moderate values of the reciprocal of the Froude number, Fr^{-1}. Third, we briefly discuss the relevance of the numerical results for flammability limits.

Influence of Gravity Strength on Flame Propagation

To focus attention on the hydrodynamic effects induced by gravity, the results presented in this section were obtained for a Lewis number of unity. Shown in Fig. 1 are the history of the deformation and expansion of the hot kernel for a relatively large value of Fr^{-1}, namely $Fr^{-1} = 100$. In the sequence of the four pictures, which pertain to $t = 0.06$, 0.96, 1.92, and 2.88, respectively, the flame is represented by a temperature contour corresponding to $\theta = 0.95$, while the arrows show the velocity field relative to a frame moving with a suitably defined average velocity of the kernel. It is seen that—as expected—the kernel experiences substantial deformation, essentially stretching in a direction perpendicular to the flow. Traditionally, this deformation is attributed [11,12] to the combined action of nonuniform pressure distribution and vorticity. The action of vorticity, the maximum of which is seen to lie at the back of the deformed kernel but close to its rim, clearly manifests itself by the observed roll-up of the flame contour. Furthermore, is seen that the flame has successfully resisted breakup in the vicinity of the symmetry axis at approximately $t = 0.96$ and later close to the rim. We note here that for larger values of Fr^{-1}, flame breakup is observed at these locations. Because of its importance to flame stretch (this will be discussed later), it is worth noting the change in curvature of the flame front at the back of the kernel. The observed tendency towards a planar flame at the back is obviously the result of the stabilizing effect of gravity there but also indicative of the weak vorticity near the axis in the fresh mixture. Finally, it is interesting to note the close similarity of our numerical results to the experimental results reported by Lovachev [13].

Figure 2 illustrates the evolution of three temporal quantities. These are, respectively, the averaged rise velocity of the hot kernel, its area projected to a plane perpendicular to the gravity force, and its equivalent radius R_{eq}, the latter being defined as the radius of a sphere having the same volume and same average density as the kernel. In the early stages, a rapid and linear increase in the rise velocity is observed. This can be attributed to the fact that in the early stages the drag forces, except the transient drag (responsible for the so-called added mass), are small compared to the gravity force. At approximately $t = 0.4$, as a consequence of the increase in the rise velocity and projected area, drag forces temporarily dominate the gravity force, leading to the observed maximum of the rise velocity, which is then followed by a decrease. At later stages, the growing volume

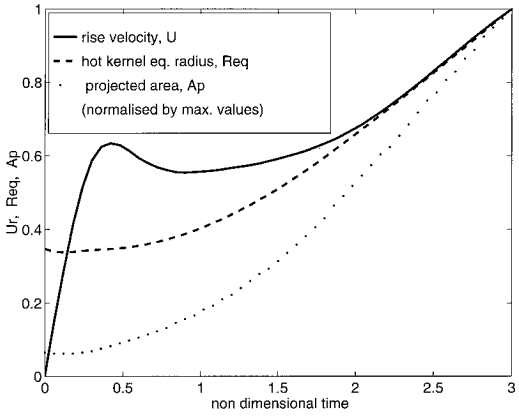

FIG. 2. Average rise velocity (solid line), hot equivalent kernel radius (dashed line), and area of the hot kernel projected on a plane perpendicular to the gravity force (dotted line) versus time. All quantities are normalized by their maximum values. Parameters as for Fig. 1.

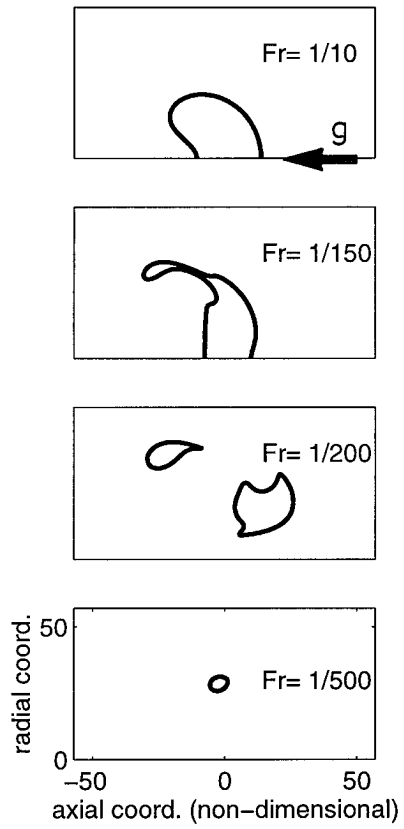

FIG. 3. Some characteristic flame shapes, illustrating the influence of Fr^{-1}. The shapes correspond—from top to bottom—to increasing values of Fr^{-1}, that is, $Fr^{-1} = 10$, $Fr^{-1} = 150$, $Fr^{-1} = 200$, and $Fr^{-1} = 500$.

of the kernel leads to a mild, continuous increase of rise velocity. Examination of the history of the equivalent radius R_{eq} of the kernel shows a delay of the onset of significant combustion. The rate of change of R_{eq} with time can be used to define a global burning velocity for a deformed, nonspherical flame kernel, which for the case of Fig. 2, for times larger than 1.5, is found to be approximately twice as big as that of a spherical kernel of same average mass.

Shown in Fig. 3 are numerically obtained flame contours for—from top to bottom—increasing values of Fr^{-1}, illustrating the influence of the gravity level on flame evolution and flame shape. The top picture ($Fr^{-1} = 10$) shows a deformed but otherwise fully connected kernel. The second picture ($Fr^{-1} = 150$) illustrates a tendency for kernel breakup, which for this case will indeed occur at a later time, whereas in the third case ($Fr^{-1} = 200$) two breakups have already occurred. Finally, the fourth picture ($Fr^{-1} = 500$) indicates that for sufficiently large values of Fr^{-1}, ring-shaped flames will form. In particular, closer inspection of the numerical results shows that in the latter case the flames form envelopes of vortex rings.

Influence of Differential Diffusion on Flame Propagation

A Potential Flow Model

We consider the case of a spherical flame ball of burned gas, of radius R, rising with velocity $\boldsymbol{U} = U\boldsymbol{e}_x$ and expanding with radial velocity $S_b = dR/dt$. The flow in the *fresh mixture* is modeled as a potential flow resulting from the superposition of a point source caused by gas expansion and a uniform flow past the ball. The velocity potential Φ associated with this flow and the velocity components in spherical coordinates, v_r and v_θ, with θ denoting the angle between $\boldsymbol{e}_x$ and $\boldsymbol{r}$, are given by

$$\Phi = -U_s \frac{R^2}{r} - \frac{R^3}{2r^3}(\boldsymbol{U}\cdot\boldsymbol{r}) \tag{7}$$

and

$$v_r \equiv \frac{\partial \Phi}{\partial r} = U_s \frac{R^2}{r^2} + \frac{R^3}{r^3} U\cos\theta$$

$$v_\theta \equiv \frac{1}{r}\frac{\partial \Phi}{\partial \theta} = \frac{R^3}{2r^3} U\sin\theta \tag{8}$$

respectively. The velocity components are relative to a frame in which the fresh gas at infinity is at rest. The quantity U_s is the radial velocity of the fresh gases at the ball surface, when the rise velocity U is zero. Using the continuity equation, it is readily found to be $U_s = \gamma S_b$, where S_b is the burning velocity relative to the burned gas. The pressure can be calculated from Bernoulli's equation, which can be written as

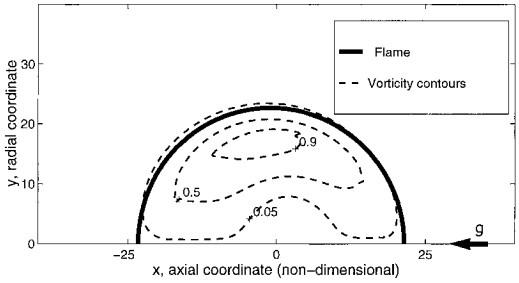

FIG. 4. Vorticity contours (dashed lines) and one flame contour (solid line) illustrating the negligibly weak vorticity of the fresh mixture. Parameters are $Fr^{-1} = 25$, $Le = 0.5$, and $R_0 = 10$. The flame contour corresponds to the iso-surface $Y = 0.95$.

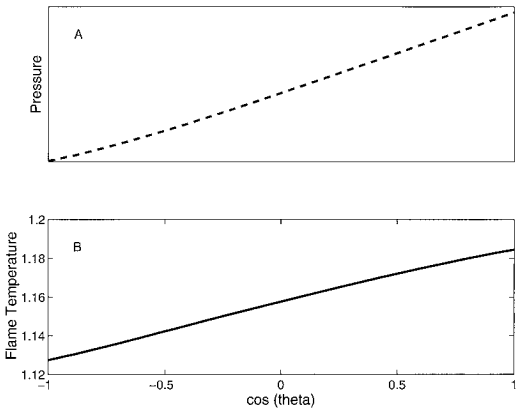

FIG. 5. Pressure distribution (a) and flame temperature θ_f (b) over the flame front shown in Fig. 4 as a function of the cosine of the polar angle with respect to e_x.

$$p + \rho \frac{\boldsymbol{v}^2}{2} + \rho \frac{\partial \phi}{\partial t} = p_\infty$$

In particular, its value at the ball surface is found to be

$$p(r = R, \theta) = \left(p_\infty - \frac{5}{8}\rho U^2 + \frac{\gamma(4 - \gamma)}{2}\rho S_b{}^2 + \gamma\rho R\frac{dS_b}{dt}\right) + \frac{9}{8}\rho U^2 \cos^2\theta + \rho\left(\frac{R}{2}\frac{dU}{dt} + \frac{3}{2}US_b\right)\cos\theta \quad (9)$$

For $S_b = 0$, Eq. (9) reduces to the classical expression for potential flow around a sphere, for $\gamma = 1$ and $U = 0$ to that of an expanding material surface [14].

An invariant form for flame stretch [15,16] is

$$\kappa \equiv \frac{1}{\Delta}\frac{d\Delta}{dt} = -\nabla \times (\boldsymbol{v} \times \boldsymbol{n})\cdot\boldsymbol{n} + (\boldsymbol{v}_{\text{flame}}\cdot\boldsymbol{n})(\nabla\cdot\boldsymbol{n}) \quad (10)$$

In Eq. (10), κ denotes the stretch, and $\boldsymbol{v}$ and $\boldsymbol{v}_{\text{flame}}$ are the fluid velocity and the flame velocity, respectively; $\boldsymbol{n}$ is the unit normal vector on the flame surface (pointing to the fresh mixture); Δ is the area of a small nonmaterial element of the flame front, which moves as a whole with the normal flame speed in the $\boldsymbol{n}$ direction while its boundary moves with the local tangential component of fluid velocity. For the flow considered herein, we have $\boldsymbol{n} = \boldsymbol{e}_r$, $\boldsymbol{v}_{\text{flame}} = \boldsymbol{U} + S_b\boldsymbol{e}_r$ and $\boldsymbol{v} = v_r\boldsymbol{e}_r + v_\theta\boldsymbol{e}_\theta$, so that according to Eq. (10) the flame stretch becomes

$$\kappa = \kappa(\theta) = \frac{2}{R}S_b + \frac{3}{R}U\cos\theta \quad (11)$$

Because of its dominant relevance to extinction and its simple dependence on κ, herein we will use the flame temperature θ_f to illustrate the influence of stretch on the flame characteristics. To this end, we use an expression derived by Matalon and Matkowski [17] (previously, equivalent expressions were derived by Clavin and Williams [18]), which in the present notations reads

$$\theta_f = \theta_f(\theta) = 1 - (\text{Le} - 1)\left[\frac{1 - \gamma}{\gamma}\int_0^{\gamma/1-\gamma}\frac{\ln(1 + x)}{x}dx\right]\cdot\kappa(\theta) \quad (12)$$

(In this formula, κ is nondimensional, the reference time being l_F^0/S_L^0.) Combination of Eqs. (11) and (12) shows the flame temperature to vary linearly with $\cos\theta$, a result whose validity will be examined in the following subsection.

As in the case of rising bubbles of moderate size [14,11], in a first approximation we may assume that the front flame surface is semispherical and that the potential-flow solution is valid there. Therefore, at least on the spherical part of the surface, the present model can be expected to be useful to explain the flame behavior for a fairly broad range of values of Fr^{-1}. However, numerical results presented later will show that the model can even be valid over the entire flame surface.

Model Validation and Interpretation of Results

The results presented in this subsection, Figs. 4–6, were obtained from the numerical solution of the governing equations, Eqs. (1) through (4) for $Fr^{-1} = 25$ and $Le = 0.5$ at a time at which the radius of the kernel has approximately doubled compared to its initial value. They can be considered as typical for weak deformation of the flame kernel as it occurs for moderate values of Fr^{-1}. In the discussion and

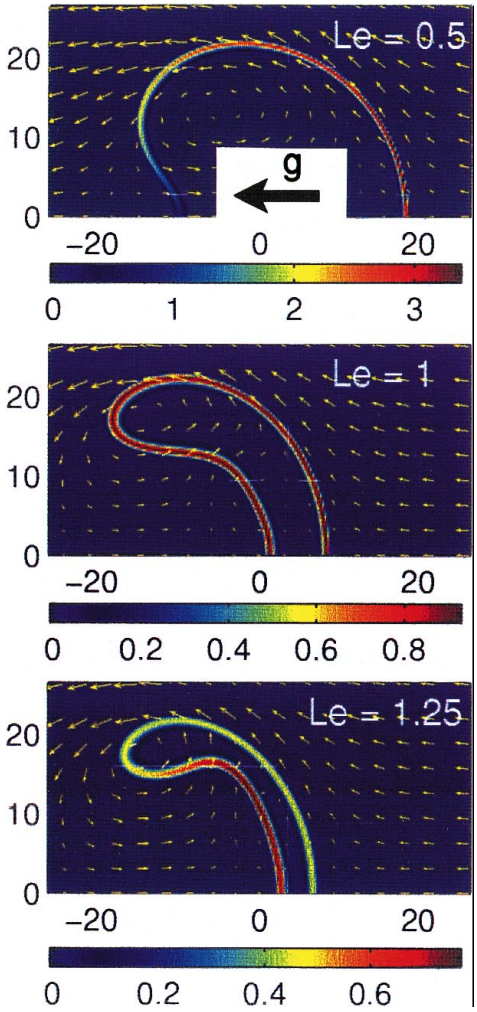

FIG. 6. Three surface plots of nondimensional reaction rate Ω, all for the same value of Fr^{-1} ($Fr^{-1} = 50$) but different Lewis numbers. From top to bottom, the Lewis number is 0.5, 1.0, and 1.25, respectively. The coordinate system is as in Fig. 1. Arrows show the velocity field relative to a frame moving with the average velocity of the hot kernel.

interpretation of the results, we will make use of the potential-flow model presented, in particular by making reference to Eqs. (9), (11), and (12).

Shown in Fig. 4 are vorticity contours (dashed lines) and a flame contour (solid line). Here, the flame contour is taken as the isosurface where $Y = 0.95$. It is clearly seen that the spherical shape of the flame is almost preserved and that to a good approximation the fresh gas can be considered as vorticity free. The latter observation can be explained as follows. First, because of flame propagation the vorticity, which is created at the flame, is quickly absorbed into the burned gas, so that the fresh gas remains essentially free of vorticity. Second, in contrast to *steady* flow around a *nonexpanding* solid sphere, the potential solution of the present *transient* problem does not necessarily exhibit an adverse pressure gradient at the back surface. This a consequence of the terms appearing in the last parentheses of Eq. (9), which in this case are dominant. That this is indeed the case is confirmed in Fig. 5a, where pressure is plotted versus cos θ, showing the linear dependence on cos θ caused by these terms. Shown in Fig. 5b is the numerically obtained flame temperature as a function of cos θ. It exhibits the linear dependence on cos θ, as is predicted by a combination of Eqs. (11) and (12). Of course, the validity of the model over the entire surface is not expected to hold at later times or for larger values of Fr^{-1}, as discussed in the following.

Figure 6 depicts three surface plots of reaction rate, all obtained numerically for a value of $Fr^{-1} = 50$ but for different Lewis numbers, namely—from top to bottom—for $Le = 0.5$, 1.0, and 1.25. The individual surface plots represent shots at times where the mass of the burned gas has grown to approximately six times its initial value. It is seen that even for high deformation of the flame kernel, the flame behavior at the front surface is as expected from stretch considerations, (i.e., at the front combustion is intensified by stretch if $Le < 1$ and weakened if $Le > 1$). Furthermore, it is seen from the first picture that for $Le < 1$ at the back surface, the reaction rate has decreased substantially, indicating the possibility of flame extinction. The second picture, which corresponds to a Lewis number of unity, shows that the flame is indeed neutral toward flame stretch, as is predicted by asymptotic analyses. From the third picture, it can be inferred that for $Le > 1$ flame extinction may occur at the front surface of the kernel.

We close this section by noting that, because of the inversion of curvature at the back, curvature there will give a negative contribution to flame stretch. However, because of recirculation of the flow at the back surface, strain there typically makes a positive contribution to flame stretch. Therefore, the situation at the back of the hot kernel should be carefully considered from case to case, taking into account the relative importance of these two contributions to flame stretch.

Concluding Remarks

Because the relative importance of gravity increases with decreasing flame speed, the results obtained herein are now discussed in connection with experimental findings, which are (mainly) concerned with flammability limits. There is an increasing

acceptance that flammability limits are only *partially* intrinsic in the sense that they are caused by kinetic effects leading to a substantial increase of the overall activation energy but that a small external perturbation is required to trigger flame extinction [19]. In the present study, complicating effects such as the increase of activation energy are not taken into account. Rather, we focus attention on the effect of gravity alone on a flame characterized by a given propagation velocity.

First, we note that the numerical results reproduce the near-limit flame shapes observed experimentally, including inversion of curvature at the back of the kernel and flame breakup [1,13,20]. Most of the predicted flame shapes are similar to classical findings on bubble shapes [12]. Second, it is interesting to mention the observation by Ronney [1,2], who experimentally studied flames in *cylindrical vessels,* that in the presence of gravity near-limit methane-air flames, which would extinguish under microgravity conditions, are still able to propagate upward. In conjunction with our results obtained in a similar geometry, this observation may be explained by the fact that $Le < 1$ for such flames and by the positive stretch at the front surface. However, Strehlow [4] reported that for upward propagating methane-air flames *in tubes*, the flammability limits are the same at normal and reduced gravity. It is tempting to conclude that the difference between the results of these authors are due to the confinement present in the tube and the difference of the flow in both cases [13].

Finally, we note that for $Le = 1$, our results show an almost perfect resistance to extinction caused by flame stretch in the gravity-induced flow. This, and the local extinction predicted herein for Lewis numbers different from unity, is in agreement with the present knowledge on stretch [18,17,21]. We further note that all flames considered in the present study, that is, flames with initial radius $R_0 = 10$, have managed to propagate at least partially, even for large values of Fr^{-1}. Total extinction of the hot initial kernel was observed only before the establishment of flame propagation in the case $Le > 1$, where a rapid breakup of the kernel was observed, a phenomenon more properly interpreted as an ignition failure. The latter situation is typically encountered in experiments for $Le > 1$, where ignition limits are found to occur before flammability limits [3].

Acknowledgments

The present study was supported by the Commission of the European Communities within the frame of the Programme "Gravity Dependent Phenomena in Combustion."

REFERENCES

1. Ronney, P. D. and Wachman, H. Y., *Combust. Flame* 62:107 (1985).
2. Ronney, P. D. and Wachman, H. Y., *Combust. Flame* 62:121 (1985).
3. Ronney, P. D., *Twenty-Second Symposium (International) on Combustion,* The Combustion Institute, Pittsburgh, 1988, p. 1615.
4. Strehlow, R. A., Kurt, A. N., and Whereley, B. L., *Twenty-First Symposium (International) on Combustion,* The Combustion Institute, Pittsburgh, 1986, p. 1899.
5. Jarosinski, J., Strehlow, R. A., and Azarbarzin, A., *Nineteenth Symposium (International) on Combustion,* The Combustion Institute, Pittsburgh, 1986, pp. 1549–1557.
6. Gieras, M. and Wolanski, P., *Archivum Combustionis* 12:1–4 (1992).
7. Hertzberg, M., *Twentieth Symposium (International) on Combustion,* The Combustion Institute, Pittsburgh, 1984, p. 1967.
8. Pelce, P. and Clavin, P., *J. Fluid Mech.* 124:219 (1982).
9. Strehlow, R. A., *Combustion Fundamentals,* 2d ed., McGraw Hill, New York, 1984.
10. Ruge, J. and Stüben, K., *Proceedings of the Multigrid Conference,* Bristol, September 1983.
11. Levich, V. G., *Physicochemical Hydrodynamics,* Prentice Hall, New York, 1962.
12. Clift, R., Grace, J. R., and Weber, M. E., *Bubbles, Drops, and Particles,* Academic Press, New York, 1978.
13. Lovachev, L. A., *Combust. Sci. Technol.* 20:209 (1979).
14. Batchelor, G. K., *An Introduction to Fluid Dynamics,* Cambridge University Press, 1967.
15. Matalon, M., *Combust. Sci. Technol.* 29:225 (1983).
16. Chung, S. H. and Law, C. K., *Combust. Flame* 55:123 (1984).
17. Matalon, M. and Matkowski, B. J., *J. Fluid Mech.* 124:239 (1982).
18. Clavin, P. and Williams, F. A., *J. Fluid Mech.* 116:000 (1982).
19. Law, C. K. and Egolfopoulos, F. N., *Twenty-Fourth Symposium (International) on Combustion,* The Combustion Institute, Pittsburgh, 1992, p. 137.
20. Andrews, G. E. and Bradley, D., *Fourteenth Symposium (International) on Combustion,* The Combustion Institute, Pittsburgh, 1973, pp. 1119–1128.
21. Law, C. K., *Twenty-Second Symposium (International) on Combustion,* The Combustion Institute, Pittsburgh, 1988, p. 1381.